

# Hysteresis in driven disordered systems: from plastic depinning to magnets

M. Cristina Marchetti<sup>1</sup> and Karin A. Dahmen<sup>2</sup>

<sup>1</sup>*Physics Department, Syracuse University, Syracuse, NY 13244*

<sup>2</sup>*Loomis Laboratory, University of Illinois at Urbana-Champaign, Urbana, IL 61801*

We study the dynamics of a viscoelastic medium driven through quenched disorder by expanding about mean field theory in  $6 - \epsilon$  dimensions. The model exhibits a critical point separating a region where the dynamics is hysteretic, with a macroscopic jump between strongly pinned and weakly pinned states, from a region where the sliding state is unique and no jump occurs. The disappearance of the jump at the critical point is described by universal exponents. As suggested in [1], the model appears to be in the same universality class as the zero-temperature random field Ising model of hysteresis in magnets.

## I. INTRODUCTION

Since the eighties the depinning of various *elastic* interfaces, ranging from domain walls in magnets to geological faults, has received great attention. Many elastic interface models with dissipative dynamics display a continuous transition from pinned to sliding at a critical driving force  $F_c$  [7,8]. Near this transition the behavior is universal on long length scales, *i.e.* it does not depend on microscopic details, but only on general properties of the system, such as symmetries, dimensions, range of interactions, and the dynamics. The sliding state is unique and no hysteresis can occur [9]. This class of systems has been studied extensively by renormalization group (RG) methods [8] and numerical simulations [10]. Meanwhile, a large body of experimental [2,3] and numerical work [4,5] has shown that many extended condensed matter systems with strong disorder exhibit a spatially inhomogeneous *plastic* response, when set into motion by an external drive [6]. In this plastic flow regime, topological defects proliferate and the system is broken up in fluid-like regions flowing around pinned solid regions. The elastic restoring forces are replaced by viscous flow on various scales [11], allowing for hysteretic response. Examples include vortex arrays in disordered superconductors, charge density waves (CDWs) in anisotropic metals, colloids, and many others. Only for weak disorder these extended systems can be described as elastic objects pulled through a quenched random medium by a uniform force  $F$ . Although several *mean-field* (MF) models of dissipative dynamics with locally underdamped relaxation have been proposed in the literature in various physical contexts [12,13,6] and shown to exhibit hysteresis, very little is known analytically about the behavior of such models in finite dimensions. This article provides first analytical (RG) results for a viscoelastic model that was introduced and previously studied in MF theory by Marchetti and collaborators [1], and makes an important contribution towards the identification of universal-

ity classes for nonequilibrium disordered systems. In [1] it was shown that in MF theory the model has a critical point, separating continuous from hysteretic dynamics. In this paper we show that in finite dimensions the behavior maps onto critical hysteresis in disordered magnets as modeled by the zero temperature non-equilibrium random field Ising model (RFIM) [14]. By showing that the two models are in fact in the same universality class we obtain the critical exponents for hysteresis in plastic flow in an expansion in  $6 - \epsilon$  dimensions.

## II. THE DRIVEN VISCOELASTIC MODEL

In Ref. [1] it is proposed that a description of shear deformations in the plastic regime may be obtained by focusing on the dynamics of coarse-grained degrees of freedom (the solid-like regions) that are allowed to slip past each other. The model of a driven viscoelastic medium is then obtained by replacing the elastic couplings of displacements in the coarse-grained model of an overdamped driven elastic medium with Maxwell-type couplings of velocities [1]. Considering, for simplicity, the overdamped dynamics of a scalar field, the equation of motion for the local displacement at discrete lattice sites  $i$ ,  $u(\mathbf{r}, t) \rightarrow u_i(t)$ , is

$$\gamma_0 \dot{u}_i = \sum_{\langle ij \rangle} \int_0^t ds \mu_{ij} e^{(t-s)/\tau} [\dot{u}_j(s) - \dot{u}_i(s)] + F + F_i(u_i), \quad (1)$$

where the dot denotes a time derivative, the summation is restricted to nearest neighbor pairs and  $\gamma_0$  is the friction. If all the nearest-neighbor elastic couplings are equal ( $\mu_{ij} = \mu \geq 0$ ), the first term on the right hand side of Eq. (1) is the discrete Laplacian in  $d$  dimensions. The second term is the homogeneous driving force,  $F$ , and  $F_i(u_i)$  denotes the pinning force arising from a quenched random potential,  $V_i(u_i)$ ,  $F_i(u_i) = -dV_i/du_i = h_i Y(u_i - \beta_i)$ ,

with  $Y(u)$  a periodic function with period 1 and  $\beta_i$  random phases uniformly distributed in  $[0, 1]$ . The random pinning forces  $h_i$  are distributed with probability  $\rho(h) = e^{-h/h_0}/h_0$ , of width  $h_0$ . The model can be used to describe pure shear deformations, where the interactions among the degrees of freedom are transverse to the direction of mean motion. As shown in [1], the integro-differential equation can be transformed into a second order differential equation, given by

$$\tau \ddot{u}_i + \left( \gamma - \tau \frac{\partial F_i}{\partial u_i} \right) \dot{u}_i = \sum_{\langle ij \rangle} \eta_{ij} [\dot{u}_j - \dot{u}_i] + F + F_i(u_i), \quad (2)$$

with  $\eta_{ij} = \mu_{ij}\tau$ . The MF critical line  $\eta_c(\tau)$  separating continuous from hysteretic dynamics was obtained in [1] and is shown in the inset of Fig. 1.

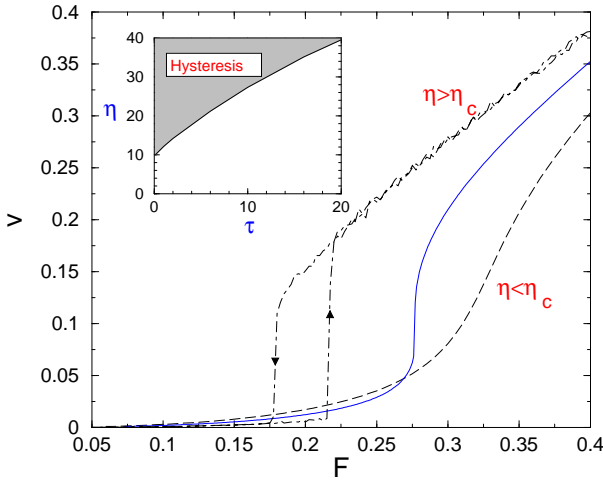


FIG. 1. Typical MF  $v - F$  curves for  $\tau = 0$  and  $\eta = 24$  (dashed-dotted),  $\eta = \eta_c = 9.745$  (solid), and  $\eta = 6$  (dashed). The inset shows the phase diagram in the  $(\eta, \tau)$  plane. The shaded area where the region where the hysteresis is hysteretic ( $\eta > \eta_c$ ) is indicated.

In this paper we consider the limit  $\tau = 0$ , with  $\eta = \mu\tau \neq 0$ , referred to as the viscous limit, and study the critical point along the  $\tau = 0$  line. The MF analysis suggests that any finite value of  $\tau$  may be irrelevant and the large scale behavior be generically described by  $\tau = 0$ . In this limit the model reduces to

$$\dot{u}_i = \sum_{\langle ij \rangle} \eta_{ij} [\dot{u}_j - \dot{u}_i] + F + F_i(u_i). \quad (3)$$

We have introduced dimensionless variables by incorporating  $\gamma_0$  in our unit of time and scaling all forces and velocities by the width  $h_0$  of the disorder distribution. The relevant dimensionless tuning parameters are then the strength  $\eta$  of the viscous coupling and the driving force,  $F$ . The MF solution of Eq. (3) for piece-wise parabolic pinning potential was obtained in [1] and is given by

$$\bar{v} = \left\langle \frac{1}{T(h_i)} \right\rangle \quad (4)$$

where  $\langle \dots \rangle$  denotes an average over disorder and  $T(h_i)$  is the period of the  $i$ -th degree of freedom (*i.e.* the time over which the displacement  $u_i$  is incremented by one),

$$T(h) = \frac{1+\eta}{h} \left[ \ln \left( \frac{2g+h}{2g-h} \right) \right], \quad \text{for } h \leq 2g, \\ T(h) = \infty, \quad \text{for } h > 2g, \quad (5)$$

with  $g = F + \eta \bar{v}$ . The various types of dynamical response are shown in Fig. 1. For strong coupling (relative to disorder),  $\eta > \eta_c$ , a marginally pinned degree of freedom pushes over its neighbors, driving a vertical hysteretic jump in the  $\bar{v} - F$  curve between strongly pinned (slowly moving) and weakly pinned (fast moving) states. For weak coupling ( $\eta < \eta_c$ ) most degrees of freedom advance independently and the  $\bar{v} - F$  curve has no macroscopic jumps. In MF the hysteresis disappears at (and below) a special value  $\eta = \eta_c$ , where the  $\bar{v} - F$  curve has a vertical slope. Preliminary results indicate the same for simulations in three dimensions (up to fluctuations). Figure 2 shows a schematic phase diagram for the dynamical model defined by Eq. (3) in the  $(F, \eta)$  plane. The MF critical point  $(F_c, \eta_c)$  is obtained from  $\chi = d\bar{v}/dF \rightarrow \infty$  and  $d^2\bar{v}/dF^2 \rightarrow \infty$ , where  $\chi$  is the static response function. As shown in Appendix A, near this critical point the velocity  $\bar{v} - v_c$ , with  $v_c = \bar{v}(\eta_c, F_c)$ , obeys a universal scaling law,

$$\bar{v} - v_c \sim |r|^\beta \mathcal{G}_\pm \left( \frac{f'}{|r|^{\beta\delta}} \right), \quad (6)$$

where the region where the hysteresis is hysteretic ( $\eta > \eta_c$ ), with  $f = F - F_c(\eta_c)$ , is a (non-universal) rotation between the control variables  $(r, f)$  and the scaling variables  $(r, f')$ . The  $\pm$  refers to the sign of  $r$ . In MF theory the critical exponents have the values  $\beta_{MF} = 1/2$  and  $\delta_{MF} = 3$ .

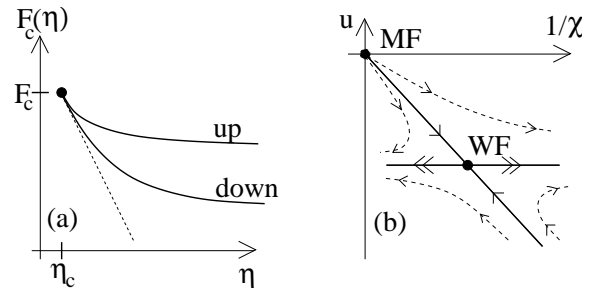


FIG. 2. Schematic MF phase diagram and RG flows. (a) The bold curve shows a vertical jump in the MF response (*i.e.* where  $d\bar{v}/dF \rightarrow \infty$ ) when the force configuration at  $F = 0$  (up); and (ii) decreased adiabatically from  $+\infty$  (down) these lines,  $(\eta_c, F_c(\eta_c))$ . (b) RG flows below 6 dimensions in the  $(\chi^{-1}, u)$  plane.  $d = 6$  and the critical behavior is obtained by linearizing around the Wilson-Fisher (WF) fixed point.

### III. BEYOND MEAN-FIELD THEORY

#### A. Formalism

Here we set up the formalism to study fluctuations about MF theory. We use the method of Martin, Siggia and Rose (MSR) to transform the stochastic equation of motion (3) into a field theory. This is done by introducing a generating functional  $Z$ , which contains the sum over the probabilities of all possible *paths* (*i.e.* microscopic configurations) which the system follows for different configurations of disorder as the force  $F$  is slowly increased. The generating functional is written as the exponential of an action, which is then renormalized perturbatively by standard methods. The MSR formalism was first adapted to driven systems by Narayan and Fisher to describe the depinning of an elastic model of CDWs [8]. It was later employed by Dahmen and Sethna to study the hysteretic response of disordered magnets [14]. Here we only give a very sketchy summary of the method and refer to the literature for details. The crucial point is to recognize that the coarse grained local velocities ( $v_i$  defined below) in the present model play the role of local magnetizations in the RFIM. The formal manipulations then follow closely those of Ref. [14], although important differences occur in the detailed calculation of the response and correlation functions.

$$S_{\text{eff}} = - \sum_{ij} \int_t dt \eta_{ij}^{-1} \hat{v}_i(t) v_j(t) + \sum_j \sum_{m,n=0}^{\infty} \frac{1}{m!n!} \int_{t_1} \dots \int_{t_{m+n}}$$

The  $u_{mn}$  are the linear and nonlinear *local* response and connected ( $\langle \rangle_c$ ) correlation functions, of the form

$$u_{mn} = \frac{\partial}{\partial \epsilon(t_{m+1})} \dots \frac{\partial}{\partial \epsilon(t_{m+n})} \langle \dot{u}(t_1) \dots \dot{u}(t_m) \rangle_{l,c}. \quad (11)$$

The suffix  $l$  in Eq. (11) indicates that the response and correlation functions are obtained by solving the MF equation with fixed *local* fields  $v_0$  and an infinitesimal perturbation,  $\eta\epsilon(t, t_1)$ , at  $t_1 < t$ ,

$$(1 + \eta)\partial_t u_j(t) = F + \eta v_{0j} + F_j(u_j) + \eta\epsilon(t, t_1). \quad (12)$$

The effective action (10) has the same structure as that of the spin model in Ref. [14], with local velocities  $v_i$  replacing local magnetizations. Note that while in the RFIM at fixed field all spins are fixed in time (in the steady state), in the CDW model each phase is subject to a quasiperiodic noise due to its coupling to the neighboring sites that move in a periodic potential even at fixed force. In the calculation done here this additional noise is averaged out and does not seem to affect the scaling results on long length scales. A detailed study whether or not it matters on long length scales in ways not captured by this approach is left to future work.

The functional  $Z$  is defined as a product of  $\delta$ -functions (one for each site), each of which imposes that the dynamics of each  $u_i$  is described at all times by the equation of motion (3). The  $\delta$ -functions are then rewritten using a standard identity, so that

$$1 \equiv Z = \int [du][d\hat{u}] J[u] e^S, \quad (7)$$

with  $\hat{u}_i$  MSR auxiliary fields. Here  $J[u]$  is a functional Jacobian chosen so that  $Z$  integrates to unity and  $S$  is an action given by

$$S = i \int_t \hat{u}_i \left[ \dot{u}_i - \sum_{\langle ij \rangle} \eta_{ij} [\dot{u}_j - \dot{u}_i] - F - F_i(u_i) \right]. \quad (8)$$

To study perturbatively fluctuations about MF theory we change variables from the  $u_i$  and  $\hat{u}_i$  to the local velocities  $v_i = (1/\eta) \sum_j \eta_{ij} \dot{u}_j$  by introducing another auxiliary field,  $\hat{v}_i$ . The MF solution  $(v_0, \hat{v}_0)$  is the saddle point of the resulting generating functional. By expanding about this solution and shifting the definition of  $v$  to  $v - v_0$ , (and absorbing a factor  $i$  in the definition), we obtain the generating functional, [8,14]

$$\bar{Z} = \int [dv][d\hat{v}] e^{S_{\text{eff}}} \quad (9)$$

with an effective action

$$u_{mn}(t_1, \dots, t_{m+n}) \hat{v}_j(t_1) \dots \hat{v}_j(t_m) v_j(t_{m+1}) \dots v_j(t_{m+n}). \quad (10)$$

#### B. Results

The response function of order  $n$  is calculated by perturbing the system with  $n$   $\delta$ -function pulses of strength  $\epsilon_1, \epsilon_2, \dots, \epsilon_n$  at  $t_1 < t_2 < \dots < t_n$ , and evaluating the response at a time  $t > t_n$ . In contrast to the case of driven CDWs [8], terms of order  $\sim e^{-\lambda T(h)}$ , with  $\lambda = h/(1+\eta)$ , cannot be neglected in the calculation, as, even when the mean velocity is very small, a fraction of degrees of freedom may be sliding freely, with corresponding large periods. Furthermore, the response must be evaluated over the entire history to obtain the correct low frequency behavior. An example of such a calculation for the simplest case of the linear response function is shown in Appendix B. Although the details of the calculation for the present model are different from the spin model, we find that the  $u_{mn}$  of the two models have indeed the same long wavelength and low frequency behavior, *i.e.* the effective actions of the two models are identical. Consequently,

the RG analysis of the viscoelastic model is the same as for the RFIM [14] and is not reproduced here. (We obtain the same  $\epsilon$ -expansion to all orders in  $\epsilon$ . Note that while the  $\epsilon$ -expansion for the *equilibrium* RFIM is controversial [17], and the  $\epsilon$ -expansion for the nonequilibrium RFIM has been mapped onto that of the equilibrium RFIM [14] to all orders in  $\epsilon$ , our main result here does not depend on the outcome of this controversy: the mapping of the plastic CDW depinning model onto the hysteretic RFIM is based on mapping the actions of the two models onto each other, by identifying the local velocities in the CDW model with the local magnetizations in the spin model. This mapping holds independently of the subsequent  $\epsilon$ -expansions for the respective critical exponents.) The critical exponents of the two systems are the same and are given in Table 1 [15]. Fourier transforming the fields  $v$  and  $\hat{v}$  in both space and time, the quadratic part of the effective action is given by

$$S_{\text{eff}}^G = - \int_{\mathbf{q}, \omega} \hat{v}(-\mathbf{q}, -\omega) [\eta \eta^{-1}(q) - u_{1,1}(\omega)] v(\mathbf{q}, \omega) + \frac{1}{2} \int_{\mathbf{q}, \omega} \hat{v}(-\mathbf{q}, -\omega) u_{2,0}(\omega) \hat{v}(\mathbf{q}, \omega), \quad (13)$$

where  $u_{1,0}$  is trivially zero because we expand around the stationary point. In the long wavelength and low frequency limit, we approximate  $\eta^{-1}(q) \approx \frac{1}{\eta} + Kq^2$  and  $u_{1,1}(\omega) \approx u_{1,1}^{\text{stat}} + i\omega a$ , where  $u_{1,1}^{\text{stat}} = \eta\nu'(g_0)/(1+\eta)$ , with  $g_0 = \eta v_0 + F$ , and  $u_{1,1}^{\text{stat}}$  and  $a$  are given in Appendix B. The correlation function is  $u_{2,0}(\omega) \approx 2\pi\delta(\omega) \left[ \langle (\frac{1}{T})^2 \rangle_h - \langle \frac{1}{T} \rangle_h^2 \right]$ . The bare propagator is given by  $G_{\hat{v}\hat{v}}(q, \omega) \approx [-i\omega a + \eta K q^2 - \chi^{-1}]$ , where  $\chi = [u_{1,1}^{\text{stat}} - 1]^{-1}$  is precisely the static response to a monotonically increasing external force calculated in MF theory. At the MF critical point  $\chi^{-1} = 0$  and the bare propagator becomes diffusive,  $G_{\hat{v}\hat{v}}(q, \omega = 0) \sim 1/q^2$ , while the correlation function is static, with  $G_{vv}(q, \omega) \sim \delta(\omega)/q^4$ . This behavior is the same as for the RFIM. In contrast, the bare propagator for driven *elastic* CDWs is diffusive also away from the critical point.

To set up an RG calculation, we need to consider terms beyond Gaussian in the action. To obtain an approximate effective action, we Fourier transform the fields in time, retain only the low frequency limit of the response functions, and then transform back to time. In the static limit, the  $u_{1,2}$  term has bare value  $u_{1,2}(\omega_1, \omega_2) \approx w$ , with  $w \sim \eta^2 \nu''(g_0)/(1+\eta)$ , and  $u_{1,3}(\omega_1, \omega_2, \omega_3) \approx u = \eta^3 \nu'''(g_0)/(1+\eta)$ . Note that  $w = 0$  at the MF critical point. We then obtain

$$S_{\text{eff}} \approx S_{\text{eff}}^G + \sum_i \int_t \left\{ \frac{w}{2} \hat{v}_i [v_i(t)]^2 + \frac{u}{6} \hat{v}_i(t) [v_i(t)]^3 \right\}, \quad (14)$$

which is identical to the effective action for the soft spin RFIM [14], with the local velocities here playing the role

of the local magnetizations in the RFIM. The generic behavior at long time and length scales is therefore identical to that of the RFIM. To perform the coarse-graining transformation, as usual we integrate out modes in the wave vector shell  $\Lambda/b < q < \Lambda$  ( $b > 1$ ), rescale coordinates as  $x = bx'$  and  $t = b^z t'$  and choose the rescaling of the fields so that the quadratic part of the action is unchanged at the critical point ( $\chi^{-1} = 0$ ). This requires  $z = 2$  and yields  $u'_{mn} = b^{[-(m+n)+2]d/2+2n} u_{mn}$ .

If  $d > 8$ , all  $u_{mn}$  other than those yielding quadratic terms in the action renormalize to zero and become irrelevant at large scales, indicating that the MF line for the onset of the vertical jump in the  $\bar{v} - F$  curve (where  $\chi^{-1} = 0$  and  $w \neq 0$ ) remains critical [15]. The MF scaling exponents are exact in this case.

Exponents	Mean-field	$\epsilon$ expansion
$\beta$	1/2	$1/2 - \epsilon/6 + \mathcal{O}(\epsilon^2)$
$1/\nu$	2	$2 - \epsilon/3 + \mathcal{O}(\epsilon^2)$
$\beta\delta$	3/2	$3/2 + 0.0833454\epsilon^2$

TABLE I: Universal exponents for the critical point discussed in the text. The exponents  $\beta$  and  $\delta$  describe how  $\bar{v}$  scales with  $F$  and  $\eta$ , respectively.  $\nu$  is the correlation length exponent.

For  $d < 8$  we need to distinguish two cases, depending on whether  $w' \sim b^{4-d/2}w$  is initially finite or zero. A bare action with  $\chi^{-1} = 0$  and  $w \neq 0$  at the onset line  $F_c(\eta)$  corresponds to the hysteretic region  $\eta > \eta_c$ . In this case the RG analysis carried out by Dahmen and Sethna for the RFIM shows that  $w$  flows to  $\infty$ , suggesting a sharp jump onset in the hysteresis loop for  $\eta > \eta_c$ . A bare action with  $\chi^{-1} = 0$  and  $w = 0$  corresponds to the critical point of interest here. If the bare  $w$  is zero, we must consider higher order terms. In particular we find that  $u' \sim b^{6-d}u$ , while all the higher order response functions are irrelevant for  $d = 6 - \epsilon$ . So  $d_c = 6$  is the upper critical dimension and for  $d > 6$  the critical exponents near  $(F_c, \eta_c)$  are given by MF theory. Below 6 dimensions,  $u$  is relevant. Corrections to the critical exponents were computed in  $6 - \epsilon$  dimensions in [14], the results are summarized in Table 1.

Many open questions remain. First, the RG calculation near  $(F_c, \eta_c)$  described here applies for  $\eta < \eta_c$  [14]. More work is needed to extend it above  $\eta_c$ , as well as for a proper understanding of the noise in this region. Secondly, we would like to study the finite range viscoelastic model for general value of  $\tau$ .

We thank Alan Middleton, Jennifer Schwarz for illuminating discussions and help with one of the figures. We also thank Jim Sethna for helpful comments. MCM was supported by NSF through grants DMR97-30678 at Syracuse and PHY99-07949 at ITP, Santa Barbara. KAD acknowledges support from the Materials Computation

Center (grant NSF-DMR 99-76550), NSF grant DMR00-72783, and an A. P. Sloan fellowship.

#### IV. APPENDIX A: MEAN-FIELD SCALING

Here we derive the scaling behavior near the MF critical point. It is convenient to rewrite the mean velocity as

$$\bar{v} = \frac{\nu(g)}{1 + \eta}, \quad (15)$$

by introducing the function  $\nu(g)$ ,

$$\nu(g) = \int_0^{2g} dh \rho(h) \frac{h}{\ln\left(\frac{2g+h}{2g-h}\right)}, \quad (16)$$

with  $\rho(h)$  the normalized distribution of pinning strengths. The MF critical point,  $\eta = \eta_c$ ,  $F = F_c$  and  $\bar{v} = v_c$ , is the point where the mean velocity curve has infinite slope. The conditions for the critical point easily are expressed in terms  $\nu(g)$  by differentiating both sides of Eq. (15) with respect to  $g$ , to obtain

$$\left(\frac{\partial \bar{v}}{\partial F}\right)_\eta \rightarrow \infty \Rightarrow \nu'(g) = \frac{1 + \eta}{\eta}, \quad (17)$$

$$\left(\frac{\partial^2 \bar{v}}{\partial F^2}\right)_\eta \rightarrow \infty \Rightarrow \nu''(g) = 0, \quad (18)$$

where the prime denotes a derivative with respect to  $g$ .

To determine the critical line  $F_c(\eta)$  where the slope of the  $(\bar{v}, F)$  curve diverges, we solve Eqs. (15), (17) and (18) for  $\eta$  near  $\eta_c$ . By expanding both sides of Eq. (15) in  $\delta g_c(\eta) = g_c(\eta) - g_c$  and  $\delta\eta = \eta - \eta_c$ , and using that  $\nu''(g_c) = 0$ , we obtain  $\delta g_c(\eta) \sim \pm \left[\frac{-2\delta\eta}{\eta_c^2 \nu_c'''}\right]^{1/2}$ , with  $\nu_c''' = \nu'''(g_c) < 0$ . We then use  $\delta F_c(\eta) = \delta g_c(\eta) - v_c \delta\eta - \eta_c \delta\bar{v}_c - \delta\eta \delta\bar{v}_c$ , expand both sides of Eq. (15) and eliminate  $\delta g_c(\eta)$  between the two equations, to obtain

$$\delta F_c(\eta) = -\frac{v_c}{1 + \eta_c} \delta\eta \pm \frac{2}{3\eta_c^2(1 + \eta_c)} \left[\frac{-2}{\nu_c'''}\right]^{1/2} (\delta\eta)^{3/2}. \quad (19)$$

Note that the critical line  $F_c(\eta)$  is rotated as compared to the critical line in the magnetic system.

To obtain the scaling function, we now write  $\bar{v}(F, \eta) = \bar{v}(F_c, \eta_c) + \delta\bar{v}$  in Eq. (15), expand around the critical point and eliminate  $\delta g$  in favor of  $\delta\bar{v}$ ,  $\delta\eta$  and  $\delta F$ . Retaining only terms up to cubic in the deviations from the critical point, we obtain a cubic equation for  $\delta\bar{v}$ , given by

$$\frac{\eta_c^4 \nu_c'''}{3!(1 + \eta_c)} (\delta\bar{v})^3 + \frac{1}{1 + \eta_c} \delta\eta \delta\bar{v} + \frac{v_c}{1 + \eta_c} \delta\eta + \delta F = 0. \quad (20)$$

We define a rotation from  $(F, \eta)$  to new scaling variables  $(F', \eta)$ , with  $F' = F + \frac{v_c}{1 + \eta_c} \eta$ . In terms of the new variables Eq. (20) becomes

$$(\delta\bar{v})^3 + \frac{6}{\eta_c^4 \nu_c'''} \delta\eta \delta\bar{v} + \frac{6(1 + \eta_c)}{\eta_c^4 \nu_c'''} \delta F' = 0, \quad (21)$$

whose solution is given by Eq. (6), with  $\mathcal{G}_\pm(x)$  the smallest real root of the cubic equation

$$\mathcal{G}_\pm^3 \pm \frac{6}{\eta_c^3 \nu_c'''} \mathcal{G}_\pm + \frac{6(1 + \eta_c)}{\eta_c^4 \nu_c'''} x = 0. \quad (22)$$

The scaling function satisfies  $\mathcal{G}_\pm(0) = \text{constant}$  and  $\mathcal{G}_\pm(x \gg 1) \sim x^{1/3}$ .

#### V. APPENDIX B: EVALUATION OF THE LINEAR RESPONSE

The linear response function  $u_{1,1}$  is obtained by perturbing the system with a  $\delta$ -function pulse of strength  $\epsilon > 0$  at time  $t_1$  and evaluating the response  $\langle \dot{u}(t) \rangle_{l,c}$  at time  $t > t_1$ ,

$$u_{1,1}(t, t_1) = \frac{\partial \langle \dot{u}(t) \rangle_{l,c}}{\partial \epsilon(t_1)}, \quad (23)$$

where  $u(t)$  is obtained by solving Eq. (12) for  $\epsilon(t, t_1) = \epsilon \delta(t - t_1)$  (to simplify the notation, we drop the subscript 0 on the local field  $v_0$  in Eq. (12)). The other local response and correlation functions can be evaluated by similar methods.

As shown in Fig. 3, the perturbation has two effects: it yields a discontinuous jump of the displacement at time  $t_1$  and it causes a shift in the “jump time”  $t_J$  where the displacement jumps between neighboring wells of the periodic pinning potential. Without loss of generality we assume  $t_J \leq t_1 \leq t_J + T$ , where  $T$  is the period defined in Eq. (5) and  $t_J$  is the jump time of the unperturbed solution.

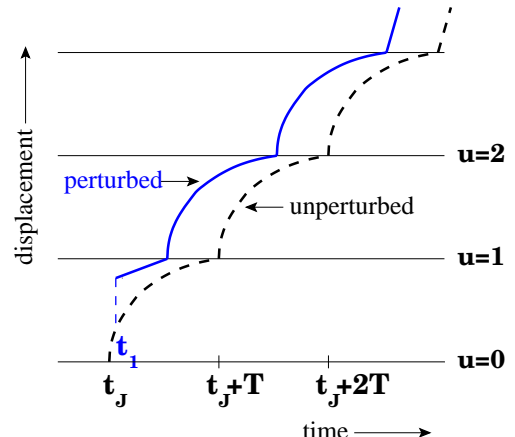


FIG. 3. Time evolution of the displacement  $u(t)$ . Both the unperturbed and perturbed solutions are shown. The perturbed solution is obtained by applying a  $\delta$ -function pulse

For  $t \geq t_1$ , the perturbed solution can be written as

$$u(t, t_1; t_J) = \Theta(t - t_1) u_{\text{unp}}(t + \delta t_J; t_J), \quad (24)$$

where  $u_{\text{unp}}(t; t_J)$  is the unperturbed solution, given by

$$u_{\text{unp}}(t; t_J) = \sum_{n=0}^{\infty} \Theta(t_J + (n+1)T - t) \Theta(t - t_J - nT) \left[ n + \frac{1 - e^{-\lambda(t-t_J-nT)}}{1 - e^{-\lambda T}} \right], \quad (25)$$

with  $\lambda = h/(1+\eta)$ . The shift in jump time  $\delta t_J$  is determined by requiring  $u(t_J - \delta t_J, t_1; t_J) = 0$ , with the result,

$$\delta t_J = -\frac{1}{\lambda} \ln (1 - \epsilon \alpha e^{-\lambda(t_J+T-t_1)}) , \quad (26)$$

$$\langle \dot{u} \rangle_{t_J} = \int_{t_1-T}^{t_1-T+t_\epsilon} \frac{dt_1}{T} \frac{\partial}{\partial t} [\Theta(t - t_1) u_{\text{unp}}(t; t_J)] + \int_{t_1-T+t_\epsilon}^{t_1} \frac{dt_1}{T} \frac{\partial}{\partial t} [\Theta(t - t_1) u_{\text{unp}}(t + \delta t_J; t_J)] . \quad (27)$$

Carrying out the integrals [18], differentiating the response with respect to  $\epsilon$  and evaluating the result at  $\epsilon = 0$ , we obtain the mean *local* linear response function,  $\chi_l(t - t_1) = u_{1,1}(t, t_1)$ , with

$$\chi_l(t) = \delta(t) \frac{\eta}{1+\eta} + \Theta(t) \left\langle \frac{\eta \lambda}{(1+\eta)T} \sum_{n=0}^{\infty} \Theta(t - nT) \Theta((n+1)T - t) e^{-\lambda(t-nT)} \left[ \left( nT - t + \frac{1}{\lambda T} \right) (e^{\lambda T} - 1) - 1 \right] \right\rangle , \quad (28)$$

where the brackets  $\langle \dots \rangle$  denote the average over  $\rho(h)$ . For  $t \geq 0$ , the response consists of the sum of a  $\delta$ -function contribution and a periodic function. The frequency dependent local response is given by

$$\begin{aligned} \tilde{\chi}_l(\omega) &= \int_0^\infty dt e^{i\omega t} \chi_l(t) , \\ &= \frac{\eta}{1+\eta} + \left\langle \frac{1}{T} \sum_s \frac{g_s}{\zeta - i(\omega - \omega_s)} \right\rangle , \end{aligned} \quad (29)$$

where the limit  $\zeta \rightarrow 0$  is intended,  $\omega_s = 2\pi s/T$ , with  $s$  an integer, and

$$g_s = -\frac{\eta \lambda e^{\lambda T}}{1+\eta} \frac{(1 - e^{-\lambda T})^2}{\lambda T} \frac{i\omega_s}{(i\omega_s - \lambda)^2} . \quad (30)$$

For small frequency, we can carry out the summation over  $s$  and find

$$\tilde{\chi}_l(\omega) \approx u_{1,1}^{\text{stat}} + i\omega a , \quad (31)$$

with

$$u_{1,1}^{\text{stat}} = \frac{\eta \nu'(g)}{1+\eta} , \quad (32)$$

and

$$\begin{aligned} a &= -\frac{\eta}{1+\eta} \left\langle \frac{1}{\lambda} + \frac{1}{2\lambda^2 T} (e^{\lambda T} - e^{-\lambda T}) \right. \\ &\quad \left. - \frac{2}{\lambda^3 T^2} (e^{\lambda T} - 1)(1 - e^{-\lambda T}) \right\rangle . \end{aligned} \quad (33)$$

if  $t_J \geq t_1 - T + t_\epsilon$ , with  $t_\epsilon = \frac{1}{\lambda} \ln(1 + \epsilon \alpha)$ , and  $\delta t_J = 0$  otherwise, with  $\alpha = \eta(e^{\lambda T} - 1)/(1 + \eta)$ .

The local response is obtained by averaging over a uniform distribution of jump times, as well as over the distribution  $\rho(h)$  of pinning strengths. The average over jump times of the perturbed velocity is given by

- [1] M. C. Marchetti, A. A. Middleton, and T. Prellberg, Phys. Rev. Lett. **85**, 1104 (2000).
- [2] S. Bhattacharya and M. J. Higgins, Phys. Rev. Lett. **70**, 2617 (1993); M. J. Higgins and S. Bhattacharya, Physica C **257**, 232 (1996).
- [3] T. Matsuda *et al.*, Science **271**, 1393 (1996); A. Tonomura, Micron **30**, 479 (1999).
- [4] A.-C. Shi and J. Berlinsky, Phys. Rev. Lett., **67**, 1926 (1991).
- [5] M. C. Faleski, M. C. Marchetti and A. A. Middleton, Phys. Rev. B **54**, 12427 (1996).
- [6] D. S. Fisher, Phys. Rep. **301**, 113 (1998).
- [7] D. S. Fisher, Phys. Rev. B **31**, 1396 (1985).
- [8] O. Narayan and D. S. Fisher, Phys. Rev. B **46**, 11520 (1992).
- [9] A. A. Middleton, Phys. Rev. Lett. **68**, 670 (1992).
- [10] A. A. Middleton, Ph.D. thesis, Princeton University, 1990; A. A. Middleton and D. S. Fisher, Phys. Rev. Lett. **66**, 92 (1991).
- [11] S. N. Coppersmith and A. J. Millis, Phys. Rev. B **44**, 7799 (1991).
- [12] S. H. Strogatz, C. M. Marcus, R. M. Westervelt, and R. E. Mirollo, Phys. Rev. Lett. **61**, 2380 (1988).
- [13] J. M. Schwartz and D. S. Fisher, Phys. Rev. Lett. **87**, 96107 (2001).
- [14] K. Dahmen and J. P. Sethna, Phys. Rev. Lett. **71**, 3222 (1993); Phys. Rev. B **53**, 14872 (1996).
- [15] The noise in the sliding state will be discussed elsewhere. It appears that the acceleration power spectrum has similar frequency scaling as in the RFIM (A. Travesset, R.A. White, and K.A. Dahmen, Phys. Rev. B, **66**, 024430 (2002)). In the MF viscoelastic model for cusped pinning potential, however, for  $\eta > \eta_c$  the slowly moving branch exhibits large velocity fluctuations not only in response to a small ramping of the force, but even spontaneously when the system is kept at a fixed driving force. This noise is not present for smooth pinning potentials.

- [16] R. da Silveira and M. Kardar, Phys. Rev. E **59**, 1355 (1999).
- [17] D.E. Feldman, Phys. Rev. Lett. **88**, 177202 (2002) and references therein.
- [18] To evaluate the second integral in Eq. (27) it is convenient to introduce the nonlinear change of variable  $y = t_J - \delta t_J(t_J)$ .